J. Am. Soc. Mass Spectrom. (2015) 26:1462–1468
DOI: 10.1007/s13361-015-1195-x

RESEARCH ARTICLE

Comparison of Internal Energy Distributions of Ions Created by Electrospray Ionization and Laser Ablation-Liquid Vortex Capture/Electrospray Ionization

John F. Cahill, Vilmos Kertesz, Olga S. Ovchinnikova, Gary J. Van Berkel

Organic and Biological Mass Spectrometry Group, Chemical Sciences Division, Oak Ridge National Laboratory, Oak Ridge, TN 37831-6131, USA

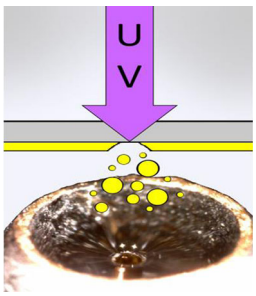

Abstract. Recently a number of techniques have combined laser ablation with liquid capture for mass spectrometry spot sampling and imaging applications. The newly developed noncontact liquid-vortex capture probe has been used to efficiently collect material ablated by a 355nm UV laser in a continuous flow solvent stream in which the captured material dissolves and then undergoes electrospray ionization. This sampling and ionization approach has produced what appears to be classic electrospray ionization spectra; however, the 'softness' of this sampling/ionization process versus simple electrospray ionization has not been definitely determined. In this work, a series of benzylpyridinium salts were employed as thermometer ions to compare internal energy distributions between electrospray ionization and the UV laser ablation/liquid-vortex capture probe electrospray combination. Measured internal energy distributions were identical between the two techniques, even with differences in laser fluence (0.7–3.1Jcm^{-2}) and when using UV-absorbing or non-UV-absorbing sample substrates. These data, along with results from the analysis the biological molecules bradykinin and angiotensin III indicated that the ions or their fragments formed directly by UV laser ablation that survive the liquid capture/electrospray ionization process were likely to be an extremely small component of the total ion signal observed. Instead, the preponderate neutral molecules, clusters, and particulates ejected from the surface during laser ablation, subsequently captured and dissolved in the flowing solvent stream, then electrosprayed, were the principal source of the ion signal observed. Thus, the electrospray ionization process used controls the overall 'softness' of this technique.

Keywords: Laser ablation, Liquid capture, Electrospray ionization, Thermometer ions, Internal energy, Surface sampling, Mass spectrometry imaging

Received: 8 January 2015/Revised: 10 March 2015/Accepted: 14 May 2015/Published Online: 27 June 2015

Introduction

Over the last number of years, laser ablation (LA) followed by liquid capture techniques have emerged for ambient spot sampling and imaging with mass spectrometry. In these methods, material is ejected by LA and collected into the charged droplets of an electrospray ionization (ESI) plume [1, 2] or, alternatively, into a suspended droplet, continuous solvent stream, or liquid microjunction [3–11]. In these latter cases, once the ablated material is captured, liquid-based methods can be used to separate components further, such as by high performance liquid chromatography (HPLC) [9, 11] or capillary electrophoresis [10], and/or the sample can be sent to a secondary ionization source such as ESI or atmospheric pressure chemical ionization (APCI) for analysis by mass spectrometry (MS).

Electronic supplementary material The online version of this article (doi:10.1007/s13361-015-1195-x) contains supplementary material, which is available to authorized users.

Correspondence to: Gary Van Berkel; *e-mail:* vanberkelgj@ornl.gov

Recently a non-contact liquid-vortex capture (LVC) probe in a vertically aligned, transmission down laser ablation geometry was introduced for the capture of ablated material [5]. The coaxial tube design of the probe with proper setting of solvent delivery and aspiration flow rates presents at the sampling end of the probe a stable liquid vortex to capture material ablated using a 355nm UV laser. The material captured in the liquid dissolves and is rapidly transported into an ESI or APCI source with the resulting ions mass analyzed. This combination of LA-LVC/ESI-MS has been shown to be capable of achieving high spatial resolution imaging (better than 10μm), and high capture efficiencies (~24%) [5]. Important, however, is understanding the magnitude of additional energy imparted to molecules in the UV-LA step and whether the unwanted fragmentation of molecules produced in this step affects the resulting LVC/ESI mass spectra. Although mass spectra presented to date indicate the overall sampling and ionization process is relatively 'soft', as little or no fragmentation is typically observed, there have been no detailed studies of the internal energy (IE) of the ions created by this technique.

Thermometer ions, based on the work of Cooks [12, 13] and later DePauw [14–16], are compounds with a simple and well known fragmentation pathway that can be used to empirically characterize the IE distributions of the ions created by a sampling/ionization process. Ions above the critical energy of dissociation are assumed to fragment. The ratio of molecular ion to fragment ion signal intensities describes the distribution of internal energies the ions created. Benzylpyridinium (BP) salts have been used to characterize 'soft' ionization techniques like ESI [14, 16], matrix-assisted laser desorption ionization (MALDI) [17–19], and many others [20–23]. In LDI and MALDI, IE distributions typically show a dependence on laser fluence when using 800nm visible and 337nm UV lasers, respectively [17–19, 24]. In contrast, for laser ablation electrospray ionization (LAESI), which utilizes a 2.94μm infrared (IR) laser, BP thermometer ion studies indicated no addition of energy compared with ESI alone [20]. This was attributed to the position of the electrospray droplets, ~12mm above the surface, which selectively acquired only neutral particulates ejected in the second phase of ablation rather than ions produced directly by the ablation process. In comparison to LAESI, LA-LVC/ESI uses harsher 355nm UV light and the probe position is closer to the substrate surface (~0.5–1mm); hence, there is the possibility that the ions created by LA-LVC/ESI could show higher IE distributions compared with ESI alone.

Herein, we report on the use of the survival yield method with BP salts [15] to characterize the IE distributions of the ions created by LA-LVC/ESI in comparison to ESI alone. The effect of laser fluence on IE distributions, with UV absorbing and non-absorbing sample substrates (DIRECTOR and glass slides, respectively) was also investigated. The data shows that the LA-LVC/ESI is a 'soft' technique, creating ions having a nearly identical IE distribution to those ions created by direct ESI. The nearly identical spectra achieved by LA-LVC/ESI and ESI analysis of the biological molecules bradykinin and angiotensin III supported these IE determinations. The secondary ESI process seems to be the predominant factor in determining the 'softness' of this LA liquid capture technique.

Experimental

ESI Source

Solutions of BP salts (1mM, 50% acetonitrile) were generously provided by Professor Edwin DePauw (Université de Liège). These solutions were diluted in 100% methanol (LC-MS Optima grade; Fisher Scientific, Pittsburg, PA, USA) to 5μM and then diluted in line further to ~30 nM. The solutions were pumped (170μLmin^{-1}) directly to a custom modified ESI probe (emitter and nebulizer capillaries, ~150μm and ~530μm, respectively) [5] in an AB Sciex TurboV ion source (AB Sciex, Concord, ON, Canada). An ESI voltage of 5000V was used. Solutions of bradykinin and angiotensin III were dissolved in 50/50/0.1v/v/v methanol/water/formic acid and diluted to a concentration of ~2μM.

Laser Ablation-Liquid Vortex Capture Probe

The LA-LVC probe and experimental setup was similar to that reported by Ovchinnikova et al. [5] as shown in Figure1. The LVC probe and laser were positioned for a vertical, transmission 'down' LA geometry. A Nd:YAG Minilight II laser (10Hz, 355nm; Santa Clara, CA, USA) was focused to a ~27μm spot on the surface of the substrate. Laser fluence was controlled using neutral density filters to achieve powers measured at the exit of the optical path of ~3.1, 2.0, and 0.7Jcm^{-2}. Solvent was delivered by an HPLC pump into the annulus of the coaxial tube probe, and then aspirated down the inner capillary into the TurboV ion source of the mass spectrometer. The LVC probe was operated at 170μLmin^{-1}, the same rate as in ESI, using 100% methanol and was positioned ~0.5mm away from the substrate. Instrument parameters (i.e., voltages, solvent flow rates, aspiration rates, etc.) were kept constant throughout ESI and LA-LVC/ESI experiments unless otherwise noted.

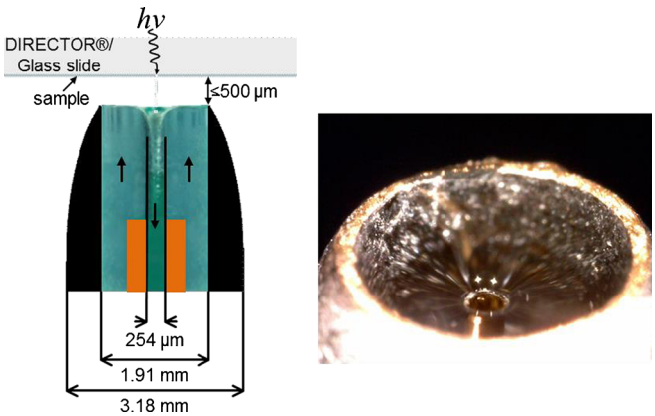

Figure 1. Cartoon of the experimental setup for LA-LVC/ESI (left) and a photograph of the sampling end of the LVC probe (right)

Mass Spectrometer

An AB Sciex 5500 Triple Quad mass spectrometer (AB Sciex) was used for the ESI and LA-LVC/ESI measurements. Mass spectrometer voltages were optimized for the BP salts and then left unchanged for all experiments. The declustering potential (DP) represents the voltage on the atmospheric sampling and was adjusted to vary the IE imparted into the ions transported through the system. Multiple reaction monitoring (MRM) scans as well as quadrupole mass spectral scans were used for the determination of survival yields. The MRM measurements yielded more reproducible results and those data are reported here.

Solutions of BP salts were deposited on slides at ~10μg cm^{-2} for glass slides and ~2μgcm^{-2} for DIRECTOR microdissection slides (Expression Pathology, Rockville, MD, USA). Mass spectral data was continually collected over ~2min while scanning the laser across the dried spot at a rate of 8μm/s. Average molecular and fragment ion signal intensities were calculated over these time intervals using OriginPro 2015 (OriginLab, Northampton, MA, USA). Signal intensities were kept between 10^4 and 10^6 counts s^{-1} for all experiments to ensure linear detector response. Within this range of intensities, survivor yields deviated by ~1% (<1 standard deviation). Similarly, solutions of bradykinin and angiotensin III were dissolved in 50/50/0.1v/v/v methanol/water/formic acid (Fisher Scientific) and deposited on glass and DIRECTOR slides at concentrations of ~150μgcm^{-2}.

Results and Discussion

Calculation of Survival Yield

The survival yield (SY) was calculated using the method of Derwa et al. [15]. The predominant unimolecular fragmentation pathway for BP salts is the C–N bond cleavage (Figure2, top) resulting in a substituted benzylium cation, $(M - 79)^+$, though other less dominant fragmentation pathways can occur [25–27]. The *para*-substituted BP salts used in the present study included BP-*p*-OCH_3, BP-*p*-CH_3, BP-*p*-F, BP-*p*-CN, and BP-*p*-NO_2 (Figure2, bottom). BP-*p*-Cl was investigated

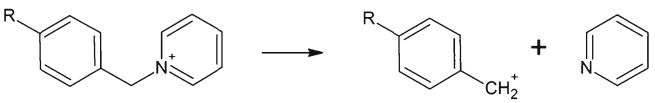

BP substituent	E_0 (eV)	*m/z* (M^+)	*m/z* (F^+)
p-OCH_3	1.51	200	121
p-CH_3	1.77	184	105
p-F	1.87	188	109
p-CN	2.1	195	116
p-NO_2	2.35	215	136

Figure 2. (top) Structure and fragmentation pathway of the benzylpyridinium cations and (bottom) fragmentation critical energies of benzylpyridinium ions used for the calculation of internal energies. Values were calculated using AM1 [16]

but had a systematically higher SY than expected from AM1 calculations. Boltzmann distribution fits with and without BP-*p*-Cl yielded the same fit parameters (just with slightly lower confidence, >0.96) as ignoring the values altogether; thus BP-*p*-Cl data was removed for subsequent data analysis. The survival yield was calculated using the formula, $SY = I(M^+)/(I(M^+) + I(F^+))$, where $I(M^+)$ and $I(F^+)$ are the signal intensities of the molecular species (M^+) and substituted benzyl cation fragment (F^+), respectively.

The IE distribution, P(E), is derived by comparing empirical SY measurements with the calculated critical energy (E_0) of unimolecular dissociation of the parent molecule. E_0 has been calculated using numerous methods [16, 28–30] and the absolute values inherently influence the resulting P(E) distribution. Previous studies have also shown that the ion source and ion optic settings in the mass spectrometer as well as the presence of other fragment ions can alter P(E) [24, 25]. As the purpose of this manuscript is to elucidate the effect of LA-LVC/ESI versus ESI on IE, accounting for the kinetic shift is unnecessary, and a relative comparison between the techniques was sufficient. Therefore, the choice of E_0 was irrelevant so long as all instrumental parameters were kept constant between experiments. All IE values reported herein are relative values rather than absolute. Survival yield values acquired in our experiments agreed with the trend in E_0 calculated using AM1 from Gabelica and De Pauw [16] and thus those values were used for the calculation of relative P(E) in this manuscript (Figure2). Two points, $E_0 = 0$, SY = 0, and $E_0 = 4$, SY = 1, were added to define the boundaries of the IE distributions. Error bars in all plots represent one standard deviation. Fragmentation of BP salts other than that forming the substituted benzylium cation had negligible abundance when the DP voltages were <200V and thus were not used in the calculation of survivor yield [25–27]. From 200 to 240V, additional fragmentation was observed but had minor impact on calculated survivor yields.

Survival Yields for ESI

Survival yield curves for different declustering potentials are shown in Figure3a. Every BP species had a sigmoidal trend in SY with DP voltage, consistent with previous findings [20, 31]. Nonlinear regression of the data using a Boltzmann's function resulted in excellent fits, with a $R^2 > 0.99$ in all cases (Figure3b). The P(E) distributions resulting from the first derivative of the curves are shown in Figure3c and mean IE (i.e. the P(E) centroid) and full width half max (FWHM) can be found in the Supplementary Information TableS1. Mean IE increased with DP voltage as expected; however, unlike in previous reports where the distribution width widened with increasing DP voltage [20, 31, 32], the widths measured here first widened then narrowed when DP voltage was increased. A significant portion of the DP voltages used here were higher than those typically used in other studies, which may have caused this discrepancy. A nearly uniform distribution of survivor yield values between 0 and 1 was obtained at DP = 160V, corresponding to a mean IE of 1.92eV, a value very similar to

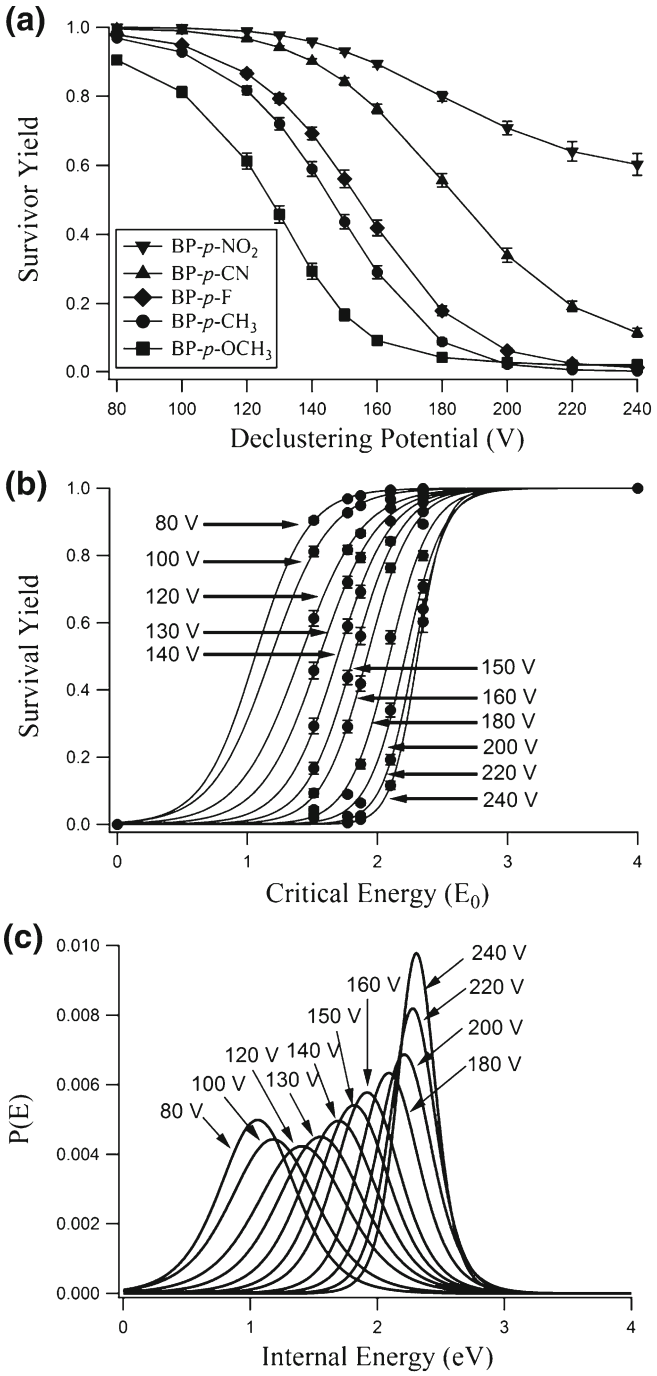

Figure 3. (**a**) Survival yields for each benzylpyridinium cation, (**b**) Boltzmann's distribution fits to survivor yields, and (**c**) corresponding internal energy distributions for ESI at different declustering potentials (DP)

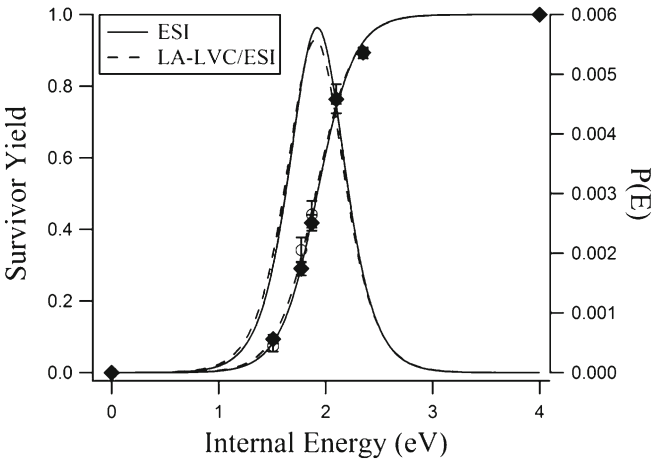

Figure 4. Comparison of the Boltzmann's and internal energy distributions between ESI (solid lines) and LA-LVC/ESI (dashed lines) using a glass slide sample substrate at a 160 V declustering potential

that reported by Nemes et al. (2.08eV) [20]. DP voltages of 120, 140, 160, and 180V were chosen for further analysis and comparison by LA-LVC/ESI.

Survival Yields for LA-LVC/ESI

The survival yields for LA-LVC/ESI at different DP voltages on glass slides are plotted in Figure4 along with the resulting P(E) at 160V. Values collected from ESI alone are also shown for reference. ESI and LA-LVC/ESI had nearly identical IE distributions peaking at 1.92±0.01 and 1.90±0.01eV, respectively. Mean internal energies determined at specific laser fluences (~3.1, 2.0, and 0.7Jcm^{-2}) for each DP value were all similar, whether using glass or DIRECTOR slides (Table1).

DIRECTOR microdissection slides contain a proprietary coating, which is highly absorbing at the UV wavelength used here, viz., 355nm. This facilitates LA for samples that are relatively non-absorbing at this wavelength. Mean internal energies obtained while using DIRECTOR and glass substrates at different laser fluences are compiled in Table1. DIRECTOR slides had a much cleaner and more uniform ablation spot than on glass slides, resulting in complete removal of material over the entire laser ablation area. Overall, very little material appeared to be ablated when using a glass slide substrate. It should be noted that the direct absorption of the UV laser by BP salts is relatively minor [19, 33]. Despite these observed ablation differences, the mean IE at each laser fluence was essentially identical to that obtained using glass slides and ESI alone. Mean internal energies and FWHM of the Gaussian distributions were within 95% error of each other. Taken together, there was no indication that the LA or the LVC had any effect on the resulting IE distribution of ions produced by the LA-LVC/ESI process.

The similarity between ESI and LA-LVC/ESI suggests that neutral projectiles ejected during the ablation process were predominantly responsible for ion signal. Nearly identical P(E) distributions between ESI and LAESI have been reported [20]; however, unlike in LAESI, the LVC probe is placed relatively close to the substrate (0.5mm compared with 12mm in LAESI) and likely can collect ions produced directly from the laser ablation/ionization process. Since ions and molecules are exposed to a liquid environment, reactions in solution could alter the decomposition product seen in ESI-MS. Full scan mass spectra were examined for the presence of additional ions (see Supplementary Information FigureS1); however no

Table 1. Mean Internal Energies and Internal Energy Distribution Widths for ESI and LA-LVC/ESI Determined at Various Declustering Potentials (DP) and Laser Fluences on Glass and DIRECTOR Slides. All values have a standard deviation of <0.02

		Mean internal energy (eV)			Full width half max (eV)		
DP (V)	Fluence (J/cm^2)	ESI	LA-LVC (Glass)	LA-LVC (DIRECTOR)	ESI	LA-LVC (Glass)	LA-LVC (DIRECTOR)
120	3.1	1.41	1.39	1.40	0.89	0.92	0.88
120	2.0	1.41	1.39	1.40	0.89	0.90	0.83
120	0.7	1.41	1.37	1.39	0.89	0.91	0.85
140	3.1	1.69	1.68	1.69	0.76	0.75	0.74
140	2.0	1.69	1.67	1.67	0.76	0.75	0.71
140	0.7	1.69	1.67	1.67	0.76	0.74	0.71
160	3.1	1.92	1.90	1.91	0.65	0.67	0.65
160	2.0	1.92	1.90	1.90	0.65	0.66	0.65
160	0.7	1.92	1.90	1.90	0.65	0.66	0.65
180	3.1	2.09	2.09	2.09	0.59	0.61	0.60
180	2.0	2.09	2.09	2.09	0.59	0.60	0.62
180	0.7	2.09	2.09	2.09	0.59	0.60	0.61

additional peaks with significant intensity were observed; thus, alternate ions, if they are formed at all, have a minor impact on the results presented. It is hypothesized that these ions may be collected by the probe, but comprise only a minor fraction of the overall ion signal with most of the signal being generated from the collected neutral particulates. Laser ablation has a low efficiency of production of ions even in the presence of a matrix (e.g., the ion/neutral ratio is ~10^{-4} for MALDI [34]) and most of the material ejected from a UV laser pulse is in the form of neutral particulates [35, 36]. The LVC probe was estimated to collect ~24% of the total material ablated; hence, it is likely that captured ions, assuming they transport through the solvent unaltered, would have negligible impact on overall ion signal [5]. Similarly, neutral fragments collected by LVC and followed by secondary ionization would have small ion intensities relative to ion intensities from the intact molecules originating from dissolved neutral particulates. With this reasoning, the laser ablation wavelength and fluence would have a negligible effect on ion signal so long as the fluence threshold for complete ablation was met.

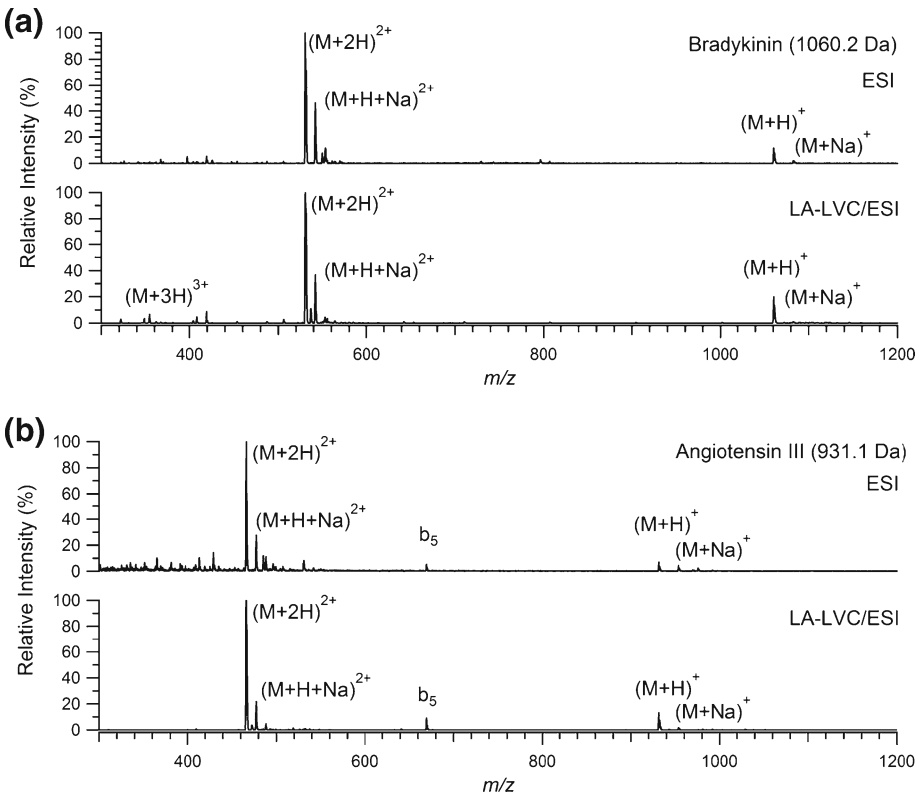

Figure 5. ESI and LA-LVC/ESI mass spectra of (**a**) bradykinin and (**b**) angiotensin III. Solutions were prepared in 50/50/0.1 v/v/v methanol/water/formic acid to 1 mM. In conventional ESI, solutions were diluted further to 2 μM using methanol for analysis. For LA-LVC/ESI, 1 μL of a 1 mM solution was spotted on a DIRECTOR slide providing a surface concentration of ~150 μg cm^{-2}

Comparison of Mass Spectra of Biomolecules Acquired using ESI and LA-LVC-ESI

Mass spectra from the direct ESI of bradykinin and angiotensin III and LA-LVC/ESI mass spectra of these same species deposited on DIRECTOR slides are shown in Figure5. The absorption of bradykinin and angiotensin III are very low at 355nm, such that when using the laser fluence used for DIRECTOR slides, but on a glass slide, no sign of ablation or mass spectral signal was observed (data not shown). For bradykinin, the $(M + H)^+$, $(M + 2H)^{2+}$, $(M + 3H)^{3+}$, $(M + Na)^+$, and $(M + H + Na)^{2+}$ can be seen at *m/z* 1061.0, 531.0, 354.3, 1083.8, and 541.9, respectively, using both ESI and LA-LVC/ESI. In the case of angiotensin III, the $(M + H)^+$ and $(M + 2H)^{2+}$ ions at *m/z* 931.6 and 466.2, respectively, were the dominant species observed. Weaker intensity ions at *m/z* 953.9 and 477.4 corresponding to $(M + Na)^+$ and $(M + H + Na)^{2+}$, respectively, and a b_5 fragment ion at *m/z* 669.4 (loss of Pro-Phe-H_2O) were also present in both the ESI and the LA-LVC-ESI mass spectra. The mass spectra collected remained similar to those shown in Figure5 even when laser fluence was varied. Overall signal intensity remained the same when scanning laser fluence, indicating that when samples were spotted on DIRECTOR slides, fluence had no impact on the observed spectra if the threshold for ablation of the coated matrix was met.

Overall, there were very minor differences between spectra acquired by ESI and LA-LVC/ESI for these two biomolecules. This is further evidence that LA-LVC/ESI is overall a 'soft' ionization technique, despite the UV laser ablation step, and is essentially comparable to ESI.

Conclusions

The results of this study show that LA-LVC/ESI is overall a 'soft' technique, creating ions having a nearly identical IE distribution to those ions created by ESI alone. The ESI process appears to be the predominant factor in determining the 'softness' of this LA liquid capture technique. The results obtained were similar to those for LAESI despite differences between the two techniques in laser wavelength (2.94μm IR and 355nm UV for LAESI and LA-LVC/ESI, respectively), laser fluence (~15 and ~0.7-3.1Jcm^{-2} for LAESI and LA-LVC/ESI, respectively), and the positioning and nature (neutral, flowing liquid versus charged droplets) of LA plume capturing liquids [20]. The use of a transmission geometry configuration and a UV absorbing DIRECTOR slide as a sample substrate in LA-LVC/ESI eliminates the need for an added UV absorbing matrix chemical (as in MALDI) or inherent water content in the sample (as in IR-LAESI) to facilitate LA. Though the transmission geometry configuration limits itself to thin films, a variety of spot sampling and imaging applications with materials like polymer or tissue sections can be imagined. Furthermore, because the probe can be connected to any liquid introduction ionization source, detection of species better suited to ionization by other molecular ionization techniques like APCI or elemental ionization using, for example, inductively coupled plasma (ICP) is possible. This range of ionization possibilities expands the overall utility of this basic LA surface sampling and ionization technique.

Acknowledgments

The authors thank Professor Edwin DePauw (Université de Liège, Belgium), for providing the benzylpyridinium salts. The AB Sciex 5500 Triple Quad mass spectrometer used in this work was provided on loan through a Cooperative Research and Development Agreement (CRADA NFE-10-02-9666) with AB Sciex. This research was supported by the U.S. Department of Energy, Office of Science, Basic Energy Sciences, Chemical Sciences, Geosciences, and Biosciences Division.

References

1. Shiea, J., Huang, M.Z., Hsu, H.J., Lee, C.Y., Yuan, C.H., Beech, I., Sunner, J.: Electrospray-assisted laser desorption /ionization mass spectrometry for direct ambient analysis of solids. Rapid Commun. Mass Spectrom. **19**, 3701–3704 (2005)
2. Nemes, P., Vertes, A.: Laser ablation electrospray ionization for atmospheric pressure, in vivo, and imaging mass spectrometry. Anal. Chem. **79**, 8098–8106 (2007)
3. Lorenz, M., Ovchinnikova, O.S., Van Berkel, G.J.: Fully automated laser ablation liquid capture surface analysis using nanoelectrospray ionization mass spectrometry. Rapid Commun. Mass Spectrom. **28**, 1312–1320 (2014)
4. Ovchinnikova, O.S., Kertesz, V., Van Berkel, G.J.: Combining transmission geometry laser ablation and a non-contact continuous flow surface sampling probe/electrospray emitter for mass spectrometry based chemical imaging. Rapid Commun. Mass Spectrom. **25**, 3735–3740 (2011)
5. Ovchinnikova, O.S., Bhandari, D., Lorenz, M., Van Berkel, G.J.: Transmission geometry laser ablation into a non-contact liquid vortex capture probe for mass spectrometry imaging. Rapid Commun. Mass Spectrom. **28**, 1665–1673 (2014)
6. Ovchinnikova, O.S., Kertesz, V., Van Berkel, G.J.: Combining laser ablation/liquid phase collection surface sampling and high-performance liquid chromatography-electrospray ionization-mass spectrometry. Anal. Chem. **83**, 1874–1878 (2011)
7. Ovchinnikova, O.S., Lorenz, M., Kertesz, V., Van Berkel, G.K.: Laser ablation sampling of materials directly into the formed liquid microjunction of a continuous flow surface sampling probe/electrospray ionization emitter for mass spectral analysis and imaging. Anal. Chem. **85**, 10211–10217 (2013)
8. Park, S.G., Murray, K.K.: Infrared laser ablation sample transfer for MALDI and electrospray. J. Am. Soc. Mass Spectrom. **22**, 1352–1362 (2011)
9. Park, S.G., Murray, K.K.: Infrared laser ablation sample transfer for on-line liquid chromatography electrospray ionization mass spectrometry. J. Mass Spectrom. **47**, 1322–1326 (2012)
10. Park, S.G., Murray, K.K.: Ambient laser ablation sampling for capillary electrophoresis mass spectrometry. Rapid Commun. Mass Spectrom. **27**, 1673–1680 (2013)
11. Kaufman, E., Smith, W., Kowalski, M., Beech, I., Sunner, J.: Electric-field-enhanced collection of laser-ablated materials onto a solvent bridge for electrospray ionization mass spectrometry. Rapid Commun. Mass Spectrom. **27**, 1567–1572 (2013)
12. Wysocki, V.H., Kenttamaa, H.I., Cooks, R.G.: Internal energy-distributions of fragmenting ions. Abstr. Pap. Am. Chem. Soc. **190**, 165–ORN (1985)
13. Wysocki, V.H., Kenttamaa, H.I., Cooks, R.G.: Internal energy-distributions of isolated ions after activation by various methods. Int. J. Mass Spectrom. Ion Process. **75**, 181–208 (1987)
14. Collette, C., De Pauw, E.: Calibration of the internal energy distribution of ions produced by electrospray. Rapid Commun. Mass Spectrom. **12**, 165–170 (1998)

15. Derwa, F., De Pauw, E., Natalis, P.: New basis for a method for the estimation of secondary ion internal energy-distribution in soft ionization techniques. Org. Mass Spectrom. **26**, 117–118 (1991)
16. Gabelica, V., De Pauw, E.: Internal energy and fragmentation of ions produced in electrospray sources. Mass Spectrom. Rev. **24**, 566–587 (2005)
17. Gabelica, V., Schulz, E., Karas, M.: Internal energy build-up in matrix-assisted laser desorption/ionization. J. Mass Spectrom. **39**, 579–593 (2004)
18. Greisch, J.F., Gabelica, V., Remacle, F., De Pauw, E.: Thermometer ions for matrix-enhanced laser desorption/ionization internal energy calibration. Rapid Commun. Mass Spectrom. **17**, 1847–1854 (2003)
19. Luo, G., Marginean, I., Vertes, A.: Internal energy of ions generated by matrix-assisted laser desorption/ionization. Anal. Chem. **74**, 6185–6190 (2002)
20. Nemes, P., Huang, H., Vertes, A.: Internal energy deposition and ion fragmentation in atmospheric-pressure mid-infrared laser ablation electrospray ionization. Phys. Chem. Chem. Phys. **14**, 2501–2507 (2012)
21. Harris, G.A., Hostetler, D.M., Hampton, C.Y., Fernandez, F.M.: Comparison of the internal energy deposition of direct analysis in real time and electrospray ionization time-of-flight mass spectrometry. J. Am. Soc. Mass Spectrom. **21**, 855–863 (2010)
22. Nefliu, M., Smith, J.N., Venter, A., Cooks, R.G.: Internal energy distributions in desorption electrospray ionization (DESI). J. Mass Spectrom. **19**, 420–427 (2008)
23. Hartmanova, L., Frycak, P., Soural, M., Turecek, F., Havlicek, V., Lemr, K.: Ion internal energy, salt tolerance and a new technical improvement of desorption nanoelectrospray. J. Am. Soc. Mass Spectrom. **49**, 750–754 (2014)
24. Milasinovic, S., Cui, Y., Gordon, R., Hanley, L.: Internal energy of thermometer ions formed by femtosecond laser desorption: implications for mass spectrometric imaging. J. Phys. Chem. C **118**, 28938–28947 (2014)
25. Barylyuk, K.V., Chingin, K., Balabin, R.M., Zenobi, R.: Fragmentation of benzylpyridinium "thermometer" ions and its effect on the accuracy of internal energy calibration. J. Am. Soc. Mass Spectrom. **21**, 172–177 (2010)
26. Morsa, D., Gabelica, V., Rosu, F., Oomens, J., De Pauw, E.: Dissociation pathways of benzylpyridinium "thermometer" ions depend on the activation regime: an IRMPD spectroscopy study. J. Phys. Chem. Lett. **5**, 3787–3791 (2014)
27. Zins, E.L., Pepe, C., Schroder, D.: Energy-dependent dissociation of benzylpyridinium ions in an ion-trap mass spectrometer. J. Mass Spectrom. **45**, 1253–1260 (2010)
28. Huang, Y., Yoon, S.H., Heron, S.R., Masselon, C.D., Edgar, J.S., Turecek, F., Goodlett, D.R.: Surface acoustic wave nebulization produces ions with lower internal energy than electrospray ionization. J. Am. Soc. Mass Spectrom. **63**, 1062–1070 (2012)
29. Naban-Maillet, J., Lesage, D., Bossée, A., Gimbert, Y., Sztáray, J., Vékey, K., Tabet, J.: Internal energy distribution in electrospray ionization. J. Mass Spectrom. **40**, 1–8 (2005)
30. Rondeau, D., Galland, N., Zins, E.L., Pepe, C., Drahos, L., Vékey, K.: Non-thermal internal energy distribution of ions observed in an electrospray source interfaced with a sector mass spectrometer. J. Mass Spectrom. **46**, 100–111 (2011)
31. Collette, C., Drahos, L., De Pauw, E., Vekey, K.: Comparison of the internal energy distributions of ions produced by different electrospray sources. Rapid Commun. Mass Spectrom. **12**, 1673–1678 (1998)
32. Pak, A., Lesage, D., Gimbert, Y., Vekey, K., Tabet, J.C.: Internal energy distribution of peptides in electrospray ionization: ESI and collision-induced dissociation spectra calculation. J. Mass Spectrom. **43**, 447–455 (2008)
33. Flanigan, P.M., Shi, F., Perez, J.J., Karki, S., Pfeiffer, C., Schafmeister, C., Levis, R.J.: Determination of internal energy distributions of laser electrospray mass spectrometry using thermometer ions and other biomolecules. J. Am. Soc. Mass Spectrom. **25**, 1572–1582 (2014)
34. Zenobi, R., Knochenmuss, R.: Ion formation in MALDI mass spectrometry. Mass Spectrom. Rev. **17**, 337–366 (1998)
35. Alves, S., Kalberer, M., Zenobi, R.: Direct detection of particles formed by laser ablation of matrices during matrix-assisted laser desorption/ionization. Rapid Commun. Mass Spectrom. **17**, 2034–2038 (2003)
36. Jackson, S.N., Mishra, S., Murray, K.K.: Characterization of coarse particles formed by laser ablation of MALDI matrixes. J. Phys. Chem. B **107**, 13106–13110 (2003)